IEEE Access
Multidisciplinary | Rapid Review | Open Access Journal

Received November 2, 2021, accepted December 20, 2021, date of publication December 23, 2021,
date of current version December 31, 2021.

Digital Object Identifier 10.1109/ACCESS.2021.3138025

Evaluation of Node-Metastasis in Sparse Underwater Acoustic Sensor Networks for Localization Under Acoustically Stratified Malicious Node Conditions

PRATEEK, (Graduate Student Member, IEEE), KUNDAN KUMAR, KRISHNA PANDEY, SAURABH CHANDRA, (Graduate Student Member, IEEE), AND RAJEEV ARYA, (Member, IEEE)
Wireless Sensor Networks Laboratory, Department of Electronics and Communication Engineering, National Institute of Technology Patna, Patna, Bihar 800005, India

Corresponding author: Prateek (prateek.ec18@nitp.ac.in)

This work was supported by the Ministry of Electronics and Information Technology, Government of India, under Grant 13(29)/2020-CC&BT.

ABSTRACT Malicious anchor node is a serious issue in underwater sensor networks. This problem gets compounded under sparse deployment scenario. To overcome this issue, the authors present a **C**ompressed **S**ensing for **M**alicious node **C**ompensation theorem (abbreviated as CS-MC Theorem) which would be applicable to underwater localization. To counter malicious node behavior, CS-MC Theorem is justified through three lemmas. For underwater acoustic propagation, a specific L_1-norm minimization method is derived. It describes the condition for unique localization of target by discretizing the target search space. Malicious node is identified by inserting the anchor nodes into the discretized grid. An insertion vector concept is introduced to determine the extent of node metastasis. Derivations are performed to prove the mathematical basis of the proposed algorithm under acoustically stratified and unstratified scenarios. Numerical results establish the feasibility of CS-MC algorithm for sparse underwater acoustic sensor network.

INDEX TERMS Underwater sensor localization, compressive acoustic sensing, sound speed stratification, insertion function, malicious anchor node.

I. INTRODUCTION

Underwater localization has come a long way since the invention of acoustic communication techniques. Acoustic signals overcome the issue of high attenuation which is faced by radio-frequency signals under water, thus it is the prime thrust area of development in terms of underwater communication. To overcome the errors of inertial navigational system (INS), a depth gauge was combined with a Kalman filter for accurate gravimetry data processing [1]. A similar approach was proposed in greater detail in [2]. Although the results were an improvement over traditional underwater sensors such as ultrashort baseline (USBL) and Doppler Velocity Log (DVL), but Kalman filter is a computationally expensive proposition. Therefore, a neural network based collaborative navigation and control is developed that leverages the power of USBL data to control the trajectory of autonomous underwater vehicles (AUVs), as formulated in [3]. To achieve target localization using underwater bearing estimates, an experimental data is collected using buoyancy Slocum glider to compensate for the drift error in [4]. However, it does not leverage cooperative localization of multiple AUVs, which is taken up by [5] in conjunction with Kalman filter fusion for underwater ranging and estimation. The next phase of improvement which is still lacking, is the prospect of sparse sensing in underwater localization, which would enable far off sensors to achieve appreciable positioning accuracy. Similar to human localization in [6], an underwater target such as a submarine may be localized using spatial clustering approach followed by edge feature based shape recognition in an effective manner.

There are certain challenges and issues in UASN Localization. In [7], underwater measurements are being taken by

The associate editor coordinating the review of this manuscript and approving it for publication was Gongbo Zhou.

forward calibration based estimation method. While 2D measurements reduce error, a new beam distribution model is formulated to simplify beam distribution characteristics. It also enables generation of templates necessary for result comparison. While both acoustic communication as well as underwater measurements are studied, the effect of node drift has altogether been bypassed since nodes are attached to seabed instead of floating ones. Had the nodes been floating, their orientation would have affected the pose-graph [8], requiring a three stage pose-graph optimization for adequate underwater localization. Location management is an important part of the localization process because it incorporates node movement into its prediction scheme. By optimizing a secondary node location using Grey Wolf Optimizer [9], both the tidal model and Node stress model are considered. However, the effect of underwater navigation remains to be addressed, which is taken up by emphasizing on the declination and inclination components of geomagnetic field [10]. This enables authors to overcome geomagnetic interference without delving into localization uncertainty concept. To deal with the relation of spectral spreading with spatial spreading due to localization uncertainty, the author in [11] has attacked localization uncertainty using a spectral graph theory concept to localize signals in the space-frequency continuum. However, there is scope of detailed discussion of regarding the spatial node distribution underwater. This scope has been addressed in [12] where the authors have computed the impact of anchor-node AUV geometry in an acoustically stratified underwater scenario on localization accuracy. Further, they have analyzed Cramer Rao Lower Bound (CRLB) of the target in an angle-constrained and range-constrained environment. A close yet unique implementation of the CRLB analysis in an underwater environment is presented in [13] because it is combined with a track-before detect algorithm in general sonar systems. Such an approach would be crucial in an underwater tracking system because sound would travel much faster in water than in air, thereby lowering the latency considerably. What would be even more useful [14] is if different placement patterns were analyzed with respect to CRLB. To further increase the localization accuracy, a hybrid approach of Time difference of arrival (TDoA) and Bearing angle of arrival (BAoA) is quite common. However, various positioning errors have been incorporated into the combined TDoA and BAoA in [15] to achieve source localization. Since they've missed out on sound speed profiling (SSP), underwater acoustic channel has been derived in presence of statistical interference in [16]. It is an important step in the underwater localization because unlike radio frequency whose impermeability is mostly limited to metallic surfaces, acoustic signal faces absorption, reflection and attenuation from any solid material surface. Therefore, in presence of a weak signal, retrieval of sparse signals by adaptive sampling has been proposed in [17] and aptly named ''Distilled Sensing''.

The domain of compressed sensing in underwater scenario is relatively new. In [18], an attempt has been made to derive CRLB to estimate Doppler shift and Time delay in a unified metric through a compressive sampling method. Compressive sampling helps to reduce the dimension of the equation, thereby simplifying the solving process. However, compressive sensing requires efficient sampling. Therefore, an efficient sampling scheme is proposed in [19] to forego the need for matrix multiplications. Direct estimation of frequency is performed without reconstruction of compressed sensing samples. A sparse Bayesian Learning framework is proposed for localization of off-grid targets [20]. By evolution of grid to formulate a sparse recovery followed by implementation of hierarchical Laplace distribution, the proposed work goes head to head with existing algorithms in terms of noise robustness and number of measurements required to retrieve the sparse target. Another advantage of compressed sensing is the reduction in the front end circuit chains. Therefore, it is preferred to use compressed sensing scheme to measure M observations than to actually use N anchor nodes to estimate the target [21]. Grid quantization that has not been applied to underwater domain but has tremendous potential, is seen in [22] To recover spectrally sparse signals from mere handful of information, requires a new algorithm such as norm based signal retrieval which uplifts the sparsity of a scenario. Authors in [23] have focused on reducing the SNR loss by improving the compressed sensing kernels using information- theoretic approach. This improvement is augmented by discretization of time delay distribution. But, underwater discretization hasn't been considered specifically, nor underwater localization. Another application of time-varying supports is dealt with the help of a proposed compressive-sensing framework called ''Potential Greedy Matching Pursuit'' where the authors have tried to relate target traces with real target positions. This technique shall be crucial in underwater systems since underwater nodes are always moving with the drift in water current. An essential requirement of sparse recovery is the block-matrix representation of the sparse signal equations which enables accurate grid-point position determination of targets. The method proposed by the authors in [24] is unique because besides reduction in sampling rate, the method also allows received signals to be represented in terms of target deviations. Therefore, weaker signals would mean greater malicious behavior of nodes, which needs to be explored in the underwater domain.

Some of the issues and challenges in Underwater Acoustic Sensor Network Localization which shapes the problem definition of the current work, are as follows.

a) *Lack of literature on underwater grid discretization*: One of the requirements of sparse sensing is the necessity for grid formation. Accurate grid formation ensures the desired correlation between actual and estimated target positions. However, to the best of authors' knowledge, discretization of grid has not been discerned individually. Since underwater sensor nodes depend upon mooring or anchoring lest they drift off, there is a need to discretize underwater grid model in order to accurately estimate the target location.

TABLE 1. Recent literature on sensing based localization applicable to underwater acoustic sensor networks.

Localization Algorithm	Type of issue addressed	Method used
C-TOL [25]	Analysis of the effect of node symmetry on the expected triangulation uncertainty	Convex-combination weighted approach, Triangulation uncertainty for node location estimation
PG-WLS [26]	Polygonal geometry with or without perturbation effects under non-coherent localization	Weighted Least squares with polygonal geometry for non-coherent localization of sensor node
FSS-FSE [7]	Forward Seabed elevation estimation in 2D space is attempted for the first time	Forward scan sonar (FSS) used with unmanned underwater vehicles (UUVs)
UL-KF Fusion [5]	Underwater positioning and ocean current estimation	Fusion of Unscented Kalman Filter and Linear Kalman Filter for cooperative localization of multiple autonomous underwater vehicles (AUVs).

b) *Malicious behavior of Underwater acoustic sensor nodes:* The underwater topology as a whole is subjected to drift due to ocean current. This unintended shift creates an offset from the prior position of the anchor nodes. This necessitates the formulation of appropriate measures to compensate for malicious behavior of the underwater nodes in order to improve localization accuracy.

c) *Lack of compressed sensing based techniques in underwater acoustic domain:* Compressed sensing is used to recover signals from incompletely received signal. Unlike radio frequency which can travel through multiple media, acoustic signals gets attenuated by slightest of obstacles, reducing the sample size of observed signals. Therefore, compressed sensing techniques which are quite helpful in land and air, should be carefully modified to suit the acoustic communication parameters of the underwater positioning system.

These issues have been actively addressed in the current work, and their highlights are outlined in section B clearly.

A. MOTIVATION AND APPLICATIONS

Acoustic communication has immense application in underwater scenarios, such as sound navigation and ranging (SONAR). It is used in devices such as ultra-short baseline (USBL), Doppler velocity log (DVL), artificial underwater landmarks (AUL) etc. UASNs have the potential to explore the underwater landscape. The prime importance of acoustic communication in underwater sensor network localization is to determine the coordinates of a target by sensing its properties such as sound speed response to an incoming beacon, the physical dimensions of the target, the mobility pattern of the target etc. Since compressed sensing promises the ability to retrieve signals from limited resources, it could be applied to underwater sensing and localization while being less demanding. Applications of UASNs are used for underwater surveying using acoustic underwater vehicles (AUVs) tectonic-plate activity monitoring, underwater geothermal vents, oil rig structural stability, submarine path planning, amongst many others. These gaps can be addressed using Compressed-sensing based underwater localization, as discussed in our work. Some of the recent works pertaining to wireless sensor network Localization have been summarized in Table 1 for visuality.

B. NOTABLE CONTRIBUTIONS

Two major shortfalls of localization using underwater acoustic networks are: first, water being a fluid, fails to contain the position of sensor nodes in their intended position for any amount of time. This leads to uneven distribution of sensor node density. While high node density doesn't hurt, sparse node density is a significant challenge to underwater localization. Second, the dependence of sound speed on other parameters of water such as temperature, pressure, salinity makes underwater acoustic communication a lot trickier. This problem gets compounded in a saline water scenario such as an ocean or brackish water lake.

To address these issues, this paper presents a compressive sensed underwater localization for spatially sparse acoustic sensor nodes. The chief contributions of this work are enumerated as follows:

a) The concept of metastasis of underwater sensor nodes is defined and derived in details to model their drifting behavior.

b) A framework of acoustic positioning recovery is proposed to approach underwater localization under metastasizing acoustic sensor nodes.

c) Sparse underwater acoustic sensor localization based on compressed sensing L1-norm minimization is presented for both unstratified as well as acoustically stratified conditions.

d) For compressed sensing to work, the bounds on insertion function are optimized in two steps; one each for stratified and unstratified acoustic channels.

C. ORGANIZATION OF PAPER

The flow of this paper is as follows: Section 1 deals with the Introduction to the UASN Localization and the necessity of Compressed sensing based sparse representation that is the main thrust area of the proposed work. Section 2 provides a thorough framework of the problem formulation pertaining to malicious node behavior under acoustic ranging techniques. The issue of node-metastasis is defined and a CS-MC Theorem is proposed to uniquely solve the UASN localization

under sparse representation and using compressed sensing approach. L1-Norm minimization is employed for realistic scenarios and compared according to different parameters. Section 3 describes a three stage justification of the proposed CS-MC Theorem through a series of statements and their mathematical proofs. Section 4 computes the performance analysis in terms of the error plot, localization ratio, correlation function and bias norm. Section 5 summarizes the findings of the work done by drawing important conclusions and takeaways from the preceding derivations and computations.

1) TABLE OF ABBREVIATIONS AND NOTATIONS

UASN	Underwater Acoustic Sensor network
CS-MC	Compressed Sensing for Malicious node Compensation
CRLB	Cramer Rao lower bound
AUV	Autonomous underwater vehicle
UAN	underwater anchor nodes
USN	underwater sensor nodes
M	Number of UANs
N	Number of USNs
$h_{n,m}$	discrete time media interface between m^{th} UAN and n^{th} USN
$\delta_{n,m}^{(l)}(j)$	Malicious behavior due to transient ocean current
$L.L.R^{p}(x_m(j))$	log likelihood ratio of $x_m(j)$
μ	malice sensitivity matrix
g	Tidal constant
ρ_{α}	Correlation function
$\mathbf{d}$	target baseline measurements
Θ	Vector which stores indices of non-zero elements
Δ	Generalized node-metastasis
$d(\alpha_i, \alpha_j)$	Standardized distance between ith and jth instance of triangulation α
$V(\alpha)$	Insertion function for triangulation α
G	Discrete lattice framework
Φ	Search space for target in the next discrete-time domain
η	Coordinates of a grid point
$g_n(\eta_0)$	Grid based tidal measurement
$\hat{m}$	Estimated number of grid points contributing to feasible solution of localization
SS_{cont}	search space in continuous domain
β	A constant in the interval (0,1)
ξ	Target parameters (such as mobility etc.)
y	Output of a discrete function
λ	Encapsulation signal
$\mathbf{R}$	discretizing vector matrix
$\boldsymbol{\gamma}(s)$	discrete partial malice vector
loc	location vector
m	orthogonal coefficient vector
s	Sensing matrix
w	Retrieval vector containing location information and orthogonal coefficient information
a, b	Distinct solution to discrete UASN positioning equations
ε	Measurement noise
$(n.A.S), (A.S)$	Acoustically unstratified path, acoustically stratified path
$C^{A.S}, C^{(n.A.S)}$	Positive constants for acoustically stratified and unstratified path, respectively
$C_g, C_g^{(A.S)}, C_g^{(n.A.S)}$	Cumulative covariances: overall, acoustically stratified, acoustically unstratified
$\hat{N}$	Matrix storing miss rate of UASN localization
$\mathbf{1}_{kk}$	Unit matrix of triangulation between kth and kth anchor node
$\beta(\alpha, \hat{\alpha})$	Bregman Projection of actual and estimated triangulation of underwater target.

II. PROBLEM FORMULATION

In this section, we attempt to lay down a broad framework of the problem formulation. The UASN consists of a transmission model as explained in equations (1) to (10). To justify the irregularities in underwater measurements, a malicious-node model is described here. Based on the type of malicious-node encountered by the UASN, the pattern of spreading of underwater sensor network is modelled through the concept of ''node-Metastasis'' in section A. ''Generalized metastasis of node'' is defined in Definition 2.1.a. Then, a mathematical approach to node-metastasis is presented with the help of a proposed theorem for Compressed Sensing for Malicious node Compensation abbreviated as the CS-MC theorem (to overcome node-metastasis in underwater scenario). The concept of CS-MC Theorem is extended with the help of Corollary 2.1.a. To prove this theorem, a Proposition 2.2.a is stated and proved in section B of acoustic positioning recovery. Then, a signal model and a noise model are stated in section C, followed by a grid based underwater malicious node model in section D. To sense the sparse sensor network, an L_1-norm minimization scheme is presented for UASN Localization in section E, which is verified in section 4. A flowchart illustrating the steps mentioned above is presented in Figure 1.

In an underwater scenario with M underwater anchor nodes (UAN) and N underwater sensor nodes (USN), the discrete time media interface between m^{th} UAN and n^{th} USN is given as

$$h_{n,m} = \left[h_{n,m}(0),\ h_{n,m}(1),\ \ldots,\ h_{n,m}(L-1)\right]^{T} \quad (1)$$

Here, the beacon containing anchor node location is broadcasted by each of the $m \in \{1, M\}$ and propagated through channel h across different kinds of direct path as well

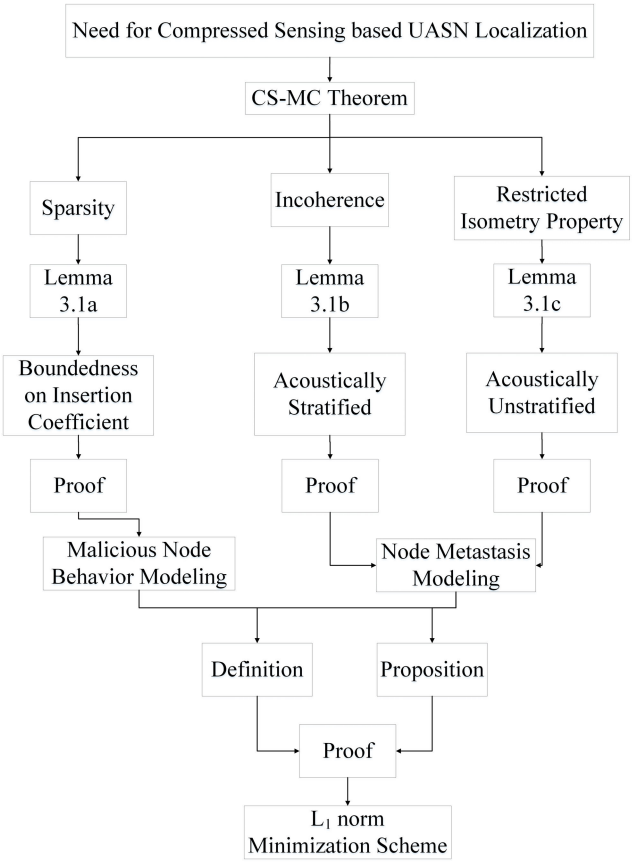

FIGURE 1. Outline of the proposed CS-MC Technique for underwater localization.

as multipath. The received beacon at n^{th} USN may be represented as

$$y_n(j) = \sum_{m=1}^{M} \sum_{l=1}^{L-1} h_{n,m}(l)\, x_m(j-l) + w_n(j), \tag{2}$$

where, the noise in the acoustic channel is $w_n(j)$ for j^{th} sample with noise variance $\frac{N_0}{2}$. Then, the average statistical parameter of the received beacon is given by

$$E(y_n(j)) = \sum\sum h_{n,m}(l)\, E(x_m(j-l)) \tag{3}$$

$$\text{var}(y_n(j)) = \sum\sum \left\|h_{n,m}(l)\right\|^2 \text{var}(x_m(j-l)) + \sigma_n^2, \tag{4}$$

where, the expectation and variance have their usual notations. Due to the various malicious node behaviors, the received beacon may be reiterated as

$$y_n(j+l) = h_{n,m}(l)\, x_m(j) + \delta_{n,m}^{(l)}(j), \tag{5}$$

where, $\delta_{n,m}^{(l)}(j)$ is the malice associated with UANs and USNs due to transient ocean currents.

$$\delta_{n,m}^{(l)}(j) = y_n(j+l) - h_{n,m}(l)\, x_m(j) \tag{6}$$

Then, the conditional probability density function of received beacon is given by

$$P(y_n(j+l)\,|x_m(j) = \pm 1)$$

$$= \frac{1}{\sqrt{2\pi\,\text{var}\left(\delta_{n,m}^{l}(j)\right)}} \times \exp\left(\frac{y(j+l) - \left(\pm h_{n,m}(l) + E\left(\delta_{n,m}^{(l)}(j)\right)\right)}{2\text{var}\left(\delta_{n,m}^{(l)}(j)\right)}\right) \tag{7}$$

To determine the estimated beacon signal received by USNs in presence of malicious node behavior, the log likelihood ratio of n^{th} received beacon is given by

$$L.L.R^p(x_m(j)) = \ln\left(\frac{P(y_m|x_m(j) = +1)}{P(y_m|x_m(j) = -1)}\right) \tag{8}$$

We approximate malice $\delta_{n,m}^{(l)}$ of underwater nodes as Gaussian distributed, therefore, the statistical parameters associated with malicious node $\delta_{n,m}^{(l)}(j)$ is given by

$$E\left(\delta_{n,m}^{(l)}(j)\right) = E\left(y_n(j+l) - h_{n,m}(l)\, E(x_m(j))\right) \tag{9}$$

$$\text{var}\left(\delta_{n,m}^{(l)}(j)\right) = \text{var}(y_n(j+l)) - \left\|h_{n,m}(l)\right\|^2 \text{var}(x_m(j)) \tag{10}$$

A. METASTASIS OF NODE

The extent to which a system of UASN drifts away in water due to water current, has been defined in this work as ''Metastasis of node'' of a UASN. To clarify this term, let us define ''Generalized metastasis of node'' first.

Definition 2.1. (Generalized Metastasis of Node): Suppose for all $\alpha_i \in \Theta$ that ρ_{α_i} satisfies the parameters $\delta_{n,m}^{(l)}(i)$ and σ_i, define the standardized distance $d(\alpha_i, \alpha_j)$ between i$^{\text{th}}$ and j$^{\text{th}}$ time instances by

$$d(\alpha_i, \alpha_j) = \frac{|\alpha_i - \alpha_j| - \delta_{n,m}^{(l)}(i) - \delta_{n,m}^{(l)}(j)}{\max(\sigma_i, \sigma_j)} \tag{11}$$

where $\delta_{n,m}^{(l)}(i)$ and $\delta_{n,m}^{(l)}(j)$ are malicious behavior of anchor nodes i and j, respectively.

Assume that the extent of metastasis of node for Θ is $\Delta > 0$ if $d(\alpha_i, \alpha_j) > |i-j|\,\Delta$ for all $\alpha_i, \alpha_j \in \Theta$ and $i \neq j$. The standardized distance $d(\alpha_i, \alpha_j)$ is measured between the edges of one triangulation α_i to the other triangulation α_j, and standardized by the level of tidal constant. This allows the extent of node-metastasis for sparsely tidal correlation function to be smaller than that of heavily tidal correlation function. The relation $d(\alpha_i, \alpha_j) > |i-j|\,\Delta$ is necessary to prevent parameters from being too bunched up together. Simply keeping $d(\alpha_i, \alpha_j) > \Delta$ does not suffice because it is weaker condition. Evidence of its weakness is visible when σ_i increases rapidly, leaving us with $d(\alpha_i, \alpha_j) \approx \Delta$ causing unrealistically small reading of node-metastasis for a given correlation function. Section A represents an example of parameters and correlation functions that satisfy the Definition 2.1.a. The upcoming CS-MC theorem shall link the extent of node-metastasis with uniform and non-uniform malicious behavior of node.

1) NODE METASTASIS IN UASN LOCALIZATION WITH NON-UNIFORM MALICIOUS BEHAVIOR

In this section, Localization of UAS Nodes is dealt with the help of correlation function ρ_α, when the correlation function ρ_α has different properties due to non-uniform malicious behavior. In order to widen the aspect of the results, the correlation function ρ_α must satisfy unique solution to UASN Localization problem for different kinds of non-uniform malicious behavior as well. That is, the correlation function shall have malicious spin and rectilinear malice of varying quantities around each vector support, as well as radial malice in presence of tidal constant. In presence of multiple malicious behavior, we need to show that the UASN localization problem is solvable depending upon a lower bound that still maintains support vector separation.

Let Θ be the vector of indices of non-zero elements of the parameter of interest. Let us assume ρ_{α_i} satisfies the radial malicious behavior condition with parameters σ_i, D_i and N_i which are different for all measurements $\alpha_i \in \Theta$. Upon changing the above parameters, the effect on corresponding correlation function is observed. By observing the correlation function it can be intuitively concluded that when σ_i and D_i are small (such as the rate of change of target travel), the corresponding correlation function ρ_{α_i} is more closely related, whereas when σ_i and D_i are large, the corresponding correlation function ρ_{α_i} is more widely related. These intuitions are supported by derivations in Sections 2 and 3. To ensure mathematical backdrop, we already defined the generalized concept of generalized node-metastasis in equation (11). Now, we state and prove Compressed Sensing for Malicious node Compensation (CS-MC) theorem which describes the node-metastasis during UASN localization under non-uniform malicious behavior.

Compressed Sensing for Malicious node Compensation (CS-MC) Theorem:

With the assumption that correlation functions concur malicious node behavior, the solution to our UASN Localization Problem is unique when the generalized node-metastasis Δ (described in Definition 2.1.a) satisfies

$$\Delta = \begin{cases} \left(\dfrac{1-k\gamma}{2\pi N_p}\right)k, & \text{for case 1} \\ 1-k\gamma, & \text{for case 2,} \end{cases} \tag{12}$$

where, case 1 corresponds to unstratified underwater acoustic network scenario, given by the expression $V''(\alpha)^{(n.A.S)} < 0$ as detailed in Lemma 3.1.c. Case 2 corresponds to the stratified acoustic scenario, given by the expression $\Delta_{\min}\|\delta_{\max^-}\|_\infty \leq \mathbf{V}(\alpha) \leq \Delta_{\max}\|\delta_{\max^+}\|_\infty$, as detailed in Lemma 3.1.e.

k = number of acoustic anchor nodes involved actively

N_p = no. of beacon signals transmitted to broadcast the anchor node locations

γ = delta between stratified and unstratified acoustic velocity.

$N_p = \frac{cT}{\lambda}$, where λ = wavelength of acoustic signals

c = velocity of acoustic signals

T = time elapsed between two consequtive beacon signal transmissions

The CS-MC Theorem is proved in Section 3. It links the concept of the minimum metastasis of node that would enable the best possible UASN Localization despite non-uniform malicious behavior. Concurrently, we may say that true localization is achieved as long as the parameters α_i are not too bunched up. The extent of metastasis of node is measured with respect to different types of malicious node behavior, which can vary as in Section D. The result matches our intuition: smaller σ_i and $\delta^{(l)}_{n,m}(i)$ result in closely related correlation function ρ_{θ_i}. As stated previously, the theorem requires a certain level of distinctness between α_i and α_j to be able to constrain the localization error of the measurement vector.

In practice, UASN Localization Problem can be approached simply by ranging methods after discretizing the continuous parameters. To extend the concept of CS-MC Theorem in the discrete domain, we present the idea through the following corollary.

Corollary 2.1.a: Let the set of indices of non-zero elements of the true location matrix be denoted by Θ. Assume that Θ is present on a known discrete lattice framework $G := \{\eta_1, \ldots \eta_m\}$ so that $\Theta \subset G$. Also assume that CS-MC theorem is fulfilled such that UASN localization is solvable in spite of non-uniform malicious node behavior. Define the search space $\boldsymbol{\eta}$ for target in the next time domain by

$$\boldsymbol{\eta} := \left[\eta^m_{R_1} \ldots \eta^m_{R_m}\right]^T, \tag{13}$$

where, m is the upper limit on the count of grid points. Then, the compressive sensing based UASN localization problem

$$\begin{aligned} &\text{minimise } (\hat{m}) \\ &\text{Subject to } y = \Phi\tilde{x} \end{aligned} \tag{14}$$

has a unique feasible solution m satisfying

$$m_j := \begin{cases} m_{threshold} \in G, & \text{under case 1} \\ m \notin G, & \text{under case 2} \end{cases} \tag{15}$$

Case 1: anchor node location coincides with grid point location

Case 2: acoustic ranging is just marred by node malice, and the outcome contains nothing useful

Here, $\tilde{x}$ is the transmitted signal, Φ is the compressed sensing matrix and y is the sensed signal for transmission of location sensing beacons.

Proof of Corollary 2.1.a: If the search space of subsequent time domain is restricted to lie on discrete lattice framework, then the estimated points as a probable solution to UASN localization would be a subset of probable solution in the continuous domain. Let the search space in continuous domain be denoted by SS_{cont}. Since SS_{cont} is a valid solution to UASN localization problem according to CS-MC Theorem, therefore, by assumption, SS_{cont} is supported on discrete lattice G, so the result follows. ■

B. PROOF OF ACOUSTIC POSITIONING RECOVERY

For the purpose of acoustic localization, the concept of unique solution to Insertion function is introduced in Proposition 2.2.a.

Proposition 2.2.a: Let $\Theta := \{\alpha_1, \ldots, \alpha_k\} \subset \mathbf{R}$ denote the support of target baseline measurements $\mathbf{d}$. Assume that for any baseline sample $\{\pm 1\}$, there is a $\tilde{v} \in \mathbb{R}$ such that the insertion matrix $V(\alpha)$ given by

$$V(\alpha) := \tilde{v}^T \eta_R^m \quad \text{satisfies } V(\alpha_i) \in k\{\pm 1\}, \tag{16}$$

where, k is the number of anchor nodes, and

$$1 - \beta \leq \frac{\|\Phi V\|_2^2}{\|V\|_2} \leq 1 + \beta, \quad \text{where } \beta \in (0, 1) \tag{17}$$

Then μ is the unique solution to our UASN Localization Problem.

Proof: For underwater scenario, the search space is continuous in nature. To enable L1-norm minimization, the search space needs to be discretized. Insertion function is used to provide a discrete template for positioning of anchor nodes and targets along the grid crossings This requires the insertion function $V(\alpha_i)$ to be bipolar non return to zero, that is, either +1 or -1, so that each unknown parameter α_i leads to corresponding insertion value $V(\alpha_i)$ that points to the next consecutive insertion (in case of +1) or to the immediate previous insertion point (in case of -1). The second condition is a standard form of the Restricted Isometry Property [27], which is essential for sparse representation. For now, insertion matrix may be understood as a collection of all the feasible solutions of the sparse sensing measurements. In our case, insertion matrix shall store the critical information about the location of target in a sparse UASN scenario. ■

Let target parameters (such as mobility etc.) be denoted by ξ. To demonstrate accurate target baseline measurement $\mathbf{d}$, we need to reaffirm the interpolation of ξ on the support Θ of target baseline measurement $\mathbf{d}$. This interpolation is facilitated by utilizing an estimated insertion function $\tilde{V}(\alpha)$ and expressing it in terms of linear combination of target coordinates.

UASN Localization Problem is the idea of estimating the underwater target location with the help of a set of underwater sensor nodes and a set of underwater anchor nodes. Underwater target location depends upon a set of parameters. Let these parameters be denoted by $x_i : x_1, \ldots x_\eta \in \mathbf{R}$. Let them be extracted from the output y of a discrete function

$$y = \sum_{i=1}^{n} \alpha_i f(x_i) \tag{18}$$

Upon sampling "y" at discrete instances $j = 1, 2, \ldots, m$, we have,

$$\begin{aligned} S &= \begin{bmatrix} y(1) & y(2) & \ldots & y(m) \end{bmatrix}^T \\ &= \sum_{i=1}^{n} \alpha_i \mathbf{f}(x_i), \end{aligned} \tag{19}$$

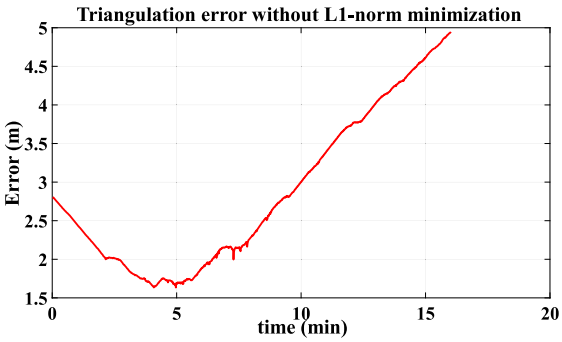

FIGURE 2. Triangulation error computed using L_2-norm (conventional method).

where, $\mathbf{f}(x_i)$ is the vector of $f(x_i)$ values for $j = 1, \ldots, m$. Formulation of UASN Localization could be approached via iterative least squares approach [28] that could be fine-tuned to run till it achieves a said performance level.

However, the difficulty in solving such a problem is that the resulting formulation is usually non-convex, and the L_2-norm may not converge to global minima [25]. An example of Triangulation localization with L_2-norm optimization is shown in Figure 2. Thus, by reducing the dimension of parameter space, we can optimize the localization problem. A suitable method would be to represent the UASN Localization Problem as a minimization of L_1-norm [29] and discretize the support of the parameter vector [30] to devise a sparse-retrieval problem. If the parameters $x_i : x_1, \ldots x_\eta \in \mathbf{R}$ are expressed as a linear combination of malicious parameter δ_{x_i}, then λ is such a signal that encapsulates the parameter information with corresponding coefficients.

$$\lambda = \sum \phi_i \delta_{x_i} \tag{20}$$

Now, representing the H variable in terms of λ and x_i

$$H = \int \mathbf{f}(x)\, \lambda dx \tag{21}$$

Although the above function is linear, it has a greater number of unknowns and fewer equations than unknowns, which makes exact retrieval near impossible. To reduce the number of unknowns to be comparable to the number of equations, we constrain the dependence of λ to a limited number of parameters. In other words, λ is sparse, therefore the retrieval method is sparse as well. The sparse UASN Localization retrieval problem may be formulated as

$$\text{Minimize } |\text{support}(\lambda)| \tag{22}$$

$$\text{Subject to } \int \mathbf{f}(x)\, \hat{\lambda} dx = H \tag{23}$$

The resulting triangulation localization with L_1-norm minimization achieves better results, as shown in Figure 4. This leads us to the signal and noise model of the framework, discussed in Section C.

C. SIGNAL MODEL AND NOISE MODEL

In underwater acoustic sensor network, we expect signal sources as follows:

1) Straight acoustic path (abbreviated as *n.A.S*) from mostly isotropic underwater regions such as unstratified waters, where the speed of sound remains constant despite change of temperature, pressure and depth. In this case, sound travels in a straight line from source to destination.
2) Stratified acoustic path (abbreviated as *A.S*) refers to the ray traced by acoustic signal under water, when the variation in depth, temperature and pressure results in the variation of speed of sound. Accordingly, a sound speed profile (SSP) [12] is maintained and the acoustic signal follows SSP to travel in a curved path.

The noise sources are also incorporated as follows:

1) Symmetric Gaussian noise, which arises due to random errors in measurement
2) Malicious Spin
3) Rectilinear malicious behavior

These conditions suggest that the location information to be retrieved from the measured vectors would be sparse and distributed over few elements. Development of suitable techniques to enable this retrieval with utmost accuracy and lowest possible computational complexity, shall lead to effective underwater ranging. Let the extent of malice be expressed as a linear combination of amplitude and phase errors. We shall show that upon discretizing the search space of malicious behavior, we shall be able to apply suitable techniques such as L_1-norm minimization, which work efficiently in the discrete domain.

D. UNDERWATER MALICIOUS BEHAVIOR MODEL

For single target localization, the determined real-valued tidal measurement $g_n(\eta_0)$ of a grid-based point (η_0) for the n^{th} retrieval at time t_n is probabilistically dependent on the partial derivative of PDF of the sensed signal y with respect to the unknown parameter α, as

$$g_n = E\left\{\frac{\partial\left(\log p_g(y)\right)}{\partial\alpha_i}\right\}^2, \tag{24}$$

where, $E\{\cdot\}$ is the expectation operator and the PDF [31] may be approximated as a joint effect of sensed area in spherical two dimensional surface (along an acoustic strata) around the target and the exponentially decaying spherical volumetric effect (along the acoustic strata as well as depth) around the target as in equation (25)

$$p_g(y) = 4\pi\left(\delta_n(\eta_0)\right) r^2 \cdot e^{-\frac{4}{3}\pi\left(\delta_n(\eta_0)\right)r^3}, \tag{25}$$

where, r is the transmission range of the sensing coverage and $\delta_n(\eta_0)$ represents the type of malicious behavior due to transient ocean current. Since the PDF is in continuous time domain, L1-norm cost function would not be applicable for minimization. Therefore, the infinite dimension of the measurement vector needs to be brought down by discretizing it along the sensing parameter s as follows:

$$\mathbf{g} = \mathbf{R}\boldsymbol{\gamma}(s), \tag{26}$$

where, $\mathbf{g}$ is the tidal measurement vector with N number of acoustic nodes measuring range for an instance of time, $\mathbf{R}$ is discretizing vector matrix with each element equaling binary values and $\boldsymbol{\gamma}(s)$ is the discrete partial malicious-node vector such that $\boldsymbol{\gamma}(s) = \left[\boldsymbol{\gamma}(s_1)\ \boldsymbol{\gamma}(s_2)\ \ldots\ \boldsymbol{\gamma}(s_l)\right]$ for 'l' number of depth points.

E. UASN LOCALIZATION VIA L1-NORM MINIMIZATION

Let us continue from equation (26) by taking a vector **loc** containing the true locations of nodes in the form of 2D-coordinates. Let the orthogonal basis vector of **loc** be given by **m**, and the sensing matrix be **s**. Then, the received signal **y** will be

$$\mathbf{y} = \mathbf{s} \cdot \mathbf{w}, \tag{27}$$

where, **w** incorporates location vector **loc** and the orthogonal coefficient vector **m**, that is, $\mathbf{w} = \mathbf{m} \cdot \mathbf{loc}$. **w** can be retrieved by L_1-norm minimization of **w** from the received signal **y** by putting equation (27) as a constraint.

$$\text{Minimize } \left\|\mathbf{w} - \mathbf{s}^{-1}\mathbf{y}\right\|_1 \tag{28}$$

$$\text{Subject to } \mathbf{w}_{rcvd} = \mathbf{s}^{-1}\mathbf{y} \tag{29}$$

Thus, summarizing section 2, malicious behavior of underwater nodes $\delta_{n,m}^{(l)}$ was dealt with in terms of sensitivity μ of localization to malicious node behavior in section A. The generalized node-metastasis Δ of Definition 2.1.a is then related to the acoustic positioning recovery in the section 2.2. Under non-uniform malicious behavior, the actual metastasis Δ undergone by the node is related to the positioning of UASN by the CS-MC theorem. To justify UASN localization by discretizing the search space of target locations Θ, a sparse sensing localization is theorized in Corollary 2.1.a which paves way for derivation of an insertion function $V(\alpha_i)$ in equation (16) of section B. The difficulty in solving the sparse UASN localization through L_2-norm is shown to be overcome when using L_1-norm minimization, as formulated in the proof of Proposition 2.2.a. After stating the signal and noise models, respectively in section C, the tidal measurement vector **g** in section D is discretized using the discretization matrix **R** to yield the desired L_1-norm minimization based sparse UASN location retrieval problem, to be solved in section 3. Solution of this expression (equation (28)) involves an in-depth look into the bounds of coefficients a and b of the insertion matrix $V(\alpha_i)$, (Lemma 3.1.a), how to maximize the insertion matrix $V(\alpha_i)$ in an unstratified (Lemma 3.1.c) as well as acoustically stratified channel scenario (Lemma 3.1b).

III. OBSERVATIONS

Besides Invertibility and Bounds on coefficients, we must focus our attention to whether or not the anchor nodes overlap the laid down grid points, that is, insertion function must

achieve optimality. For that, we verify boundation condition, and approach the optimality criteria in two steps, as illustrated in Lemma 3.1.a. The bounds on acoustically stratified and unstratified channel compel two more stages, one, to arrive at $|\mathbf{V}(\alpha)| < 1$, and second, to justify local maxima of $\mathbf{V}(\alpha)$. Lemma 3.1.b proves the former by utilizing Perron-Frobenius Theorem [32] for an acoustically stratified channel, whereas Lemma 3.1.c takes the assistance of Bregman Projection [33] to prove the latter in case of an unstratified channel.

A. JUSTIFICATION OF CS-MC THEOREM

To explain the ramifications of boundedness of coefficients a and b on the insertion function $\mathbf{V}(\alpha)$, we state and prove Lemma 3.1.a. The bounds on insertion matrix $\mathbf{V}(\alpha)$ in the specific case of acoustically stratified channel is stated and proved in Lemma 3.1.b, while the bounds on insertion matrix $\mathbf{V}(\alpha)$ in the case of acoustically unstratified channel is stated and proved in Lemma 3.1.c.

Lemma 3.1.a: Let the insertion function $\mathbf{V}(\alpha)$ consisting of coefficients a and b be bounded. Then at points of insertion α, $\mathbf{V}(\alpha)$ attains local maxima, that is, $\mathbf{V}''(\alpha) < 0$ and $|\mathbf{V}(\alpha)| < 1$.

Proof of Lemma 3.1.a: Proof of bounds on insertion matrix can be carried out in two stages: First, we show the general expression of $\mathbf{V}(\alpha)$ is less than one in case of acoustically stratified path. Next, we prove that insertion function $\mathbf{V}(\alpha)$ achieves a local maximum in case of acoustically straight channel. To obtain the overall insertion function, we utilize triangle inequality condition [34] to unify equation of acoustically stratified $\mathbf{V}(\alpha)^{(A.S)}$ as well as unstratified scenario $\mathbf{V}(\alpha)^{(n.A.S)}$, as shown:

$$\left|\mathbf{V}(\alpha)^{unified}\right| = \mathbf{V}(\alpha)^{(A.S)} + \mathbf{V}(\alpha)^{(n.A.S)} \tag{30}$$

$\mathbf{V}(\alpha)$ is expressed as a combination of coefficients in a manner similar to the sum of terms of the derivative of the covariance function with respect to the unknown parameter α. To start, two coefficients a and b are combined in an L∞-norm with the covariance $C_g^{(A.S)}$ in acoustically stratified medium, and the first order differential $\frac{\partial C_g^{(A.S)}}{\partial \alpha}$ such that the coefficients describe the discrete grid closely.

$$\mathbf{V}(\alpha)^{(A.S)} = \|a\|_\infty C_g^{(A.S)} + \|b\|_\infty \frac{\partial C_g^{(A.S)}}{\partial \alpha} \tag{31}$$

A similar approach as equation (31) for the acoustically unstratified channel (denoted by $n.A.S$) is given by equation (32) as follows

$$\text{and, } \mathbf{V}(\alpha)^{(n.A.S)} = \|a\|_\infty C_g^{(n.A.S)} + \|b\|_\infty \frac{\partial C_g^{(n.A.S)}}{\partial \alpha} \tag{32}$$

The combination of stratified as well as unstratified insertion function is expressed as $\mathbf{V}(\alpha)^{unified}$, as shown in equation (33).

$$\Rightarrow \left|\mathbf{V}(\alpha)^{unified}\right|$$

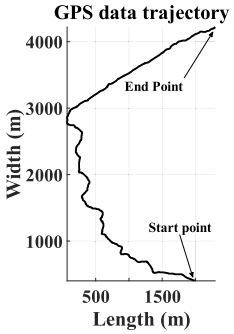

FIGURE 3. Target trajectory representation with GPS coordinates for actual positioning information.

$$= \|a\|_\infty C_g^{(A.S)} + \|b\|_\infty \frac{\partial C_g^{(A.S)}}{\partial \alpha} + \|a\|_\infty C_g^{(n.A.S)} + \|b\|_\infty \frac{\partial C_g^{(n.A.S)}}{\partial \alpha} \tag{33}$$

Therefore, the optimum value of insertion function is determined by deriving the second order derivative of the insertion function in equation (34)

$$\begin{aligned}\mathbf{V}''(\alpha)^{unified} &= \mathbf{V}''(\alpha)^{(A.S)} + \mathbf{V}''(\alpha)^{(n.A.S)} \\ &= (1 - \|a - b\|_\infty)\,\tilde{C''}_g^{(A.S)} + \|b\|_\infty \tilde{C''}_g^{(A.S)} \\ &\quad + \|a\|_\infty \tilde{C''}_g^{(n.A.S)} + \|b\|_\infty \tilde{C''}_g^{(n.A.S)}\end{aligned} \tag{34}$$

A floating sensor node is subject to node drift due to water current. Therefore, the GPS coordinates taken as a proof of actual locations help to determine the error during estimation. One such path trajectory is shown in Figure 3 to denote the start point and the end point positioning measurement for a floating target. To justify the bounds on $|\mathbf{V}(\alpha)|$ in an acoustically stratified channel, we state and prove Lemma 3.1.b as follows:

Lemma 3.1.b: Let the insertion vector $\mathbf{V}(\alpha)$ whose coefficients a and b are bounded, be placed in an acoustically stratified channel with minimum and maximum metastasis of node denoted by $\Delta_{\min}$ and $\Delta_{\max}$, respectively, and the effect of the maximum possible malicious behavior in the additive and subtractive sense be denoted by $\delta_{\max^+}$ and $\delta_{\max^-}$, respectively. Then, the bounds on the insertion vector $\mathbf{V}(\alpha)$ is given by the relation (35)

$$\Delta_{\min} \|\delta_{\max^-}\|_\infty \leq \mathbf{V}(\alpha) \leq \Delta_{\max} \|\delta_{\max^+}\|_\infty \tag{35}$$

Proof of L3.1.b: Consider the minimization problem

$$V(\alpha) := \min\left\{x^T \hat{N} x\right\} \tag{36}$$

Subject to constraints

$$0 \leq x \tag{37}$$

$$\|x\|_2 = \|V(\alpha)\|_2 \tag{38}$$

where, x is a column vector, and $\hat{N}$ is a semidefinite matrix. We have $1 \geq \sqrt{V(\alpha)}$, where equality may be achieved keeping Perron-Frobenius Theorem [32] into consideration

for the upper bounds of (35). By replacing x with underwater anchor nodes UAN such that $UAN = \left[an_1 \; an_2 \; \ldots \; an_\rho \right]^T$, where an_ρ stands for the presence of ρ^{th} anchor node responsible for ranging and measurement of target, we also have $(UAN)_{kk}^2 = \|V(\alpha)\|_2^2 - \sum_{i \neq k} (UAN)_i^2$ which broadly specifies the difference between insertion vector grid, and i^{th} malicious UAN location as the requirement for placement of $k^{th} UAN$ such that the malicious effect of i^{th} UAN is compensated safely. Starting with $\hat{N} = \mathbf{1}$ as a unit vector matrix and hence,

$$\begin{aligned}(UAN)^T (\mathbf{1}) (UAN) &= \mathbf{1}_{kk} \|V(\alpha)\|_2^2 + \sum (\mathbf{1}_{ii} - \mathbf{1}_{kk}) (UAN)_i^2 \\ &\quad + \sum_{i \neq k} \sum_{k} \mathbf{1}_{ik} (UAN)_i (UAN)_k \\ &\geq (UAN)_{kk} \|V(\alpha)\|_2^2 \end{aligned} \tag{39}$$

which proves $|V(\alpha)| \leq 1$ in the acoustically stratified channel.

To state and prove that $V''(\alpha) < 0$ in acoustically unstratified channel scenario, we have Lemma 3.1.c as follows:

Lemma 3.1.c: Let $V(\alpha)^{(n.A.S)}$ be the insertion matrix in the region of no acoustic stratification. Then, $V''(\alpha)^{(n.A.S)} < 0$.

Proof of Lemma 3.1.c: Let the fitness function of coefficients a and b be denoted by $\mathbf{U}(\alpha)$ such that the Lagrangian of Bregman Projection [35] $\beta(\alpha, \hat{\alpha})$ be given by

$$\lambda(R, M) = \beta(\alpha, \hat{\alpha} R) - tr\left(M^T R\right), \tag{40}$$

where, $\lambda(\cdot)$ denotes Lagrange's cost function and $tr(\cdot)$ denotes trace of vector matrix. Taking first differential of Lagrange's cost function, we have

$$\frac{\partial \{\lambda\}}{\partial R} = 0 \tag{41}$$

$$\begin{aligned}&\frac{\partial \left\{\beta(\alpha, \hat{\alpha} R) - tr\left(M^T R\right)\right\}}{\partial R} = 0 \\ &\Rightarrow \frac{\partial \left\{\beta(\alpha, \hat{\alpha} R)\right\}}{\partial R} = \frac{\partial tr\left(M^T R\right)}{\partial R} \\ &= M \\ &\Rightarrow \sum_i \begin{bmatrix} -\alpha_i \mathbf{U}'(\alpha \arg\min(\beta))_i \\ -\alpha_i \mathbf{U}''(\alpha \arg\min(\beta))_i \left(\alpha_i - \left(\alpha \arg\min(\beta)_i\right)\right) \\ +\mathbf{U}'(\alpha \arg\min(\beta))_i \alpha_i \end{bmatrix} \\ &= M \\ &\Rightarrow \sum_i -\left[\alpha_i \mathbf{U}''(\alpha \arg\min(\beta))_i \left(\alpha_i - \left(\alpha \arg\min(\beta)_i\right)\right)\right] \\ &= M \end{aligned} \tag{42}$$

Therefore, $\left[\mathbf{U}''(\alpha \arg\min(\beta)) \odot (\alpha - (\alpha \arg\min(\beta)))\right]^T \alpha = -M^T \leq 0 \Rightarrow V''(\alpha) \leq 0$, where,

$$V''(\alpha) = \left[\mathbf{U}''(\alpha \arg\min(\beta)) \odot (\alpha - (\alpha \arg\min(\beta)))\right]^T \alpha \tag{43}$$

$\odot$ is the elementwise multiplication operator, and it holds true when $\alpha - (\alpha \arg\min(\beta)) = \mathbf{1}$.

Thus,

$$\begin{aligned}\mathbf{V}''(\alpha)^{(n.A.S)} &= \left[\mathbf{U}''(\alpha \arg\min(\beta)) \odot \mathbf{1}\right]^T \alpha \\ &= \mathbf{U}''(\alpha \arg\min(\beta))^T \alpha \\ &\Rightarrow V''(\alpha)^{(n.A.S)} < 0 \end{aligned} \tag{44}$$

which shows that the insertion function has a local maxima in case of acoustically unstratified channel.

Summarizing section 3, it has been shown that under the conditions such as sparsity, boundedness and invertibility of coefficients a and b, sensing matrix $\mathbf{s}$ and insertion matrix $V(\alpha)$, compressed sensing based retrieval of UASN localization is feasible.

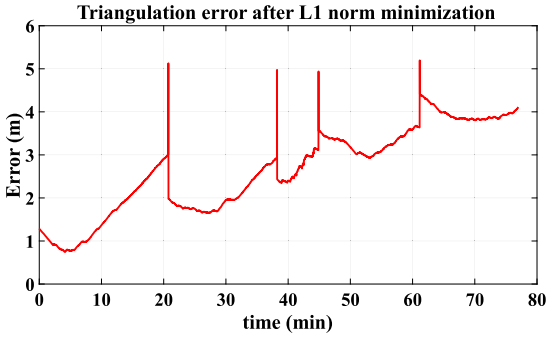

FIGURE 4. Triangulation based localization using L_1-norm minimization.

IV. SIMULATION RESULTS

Simulations were performed by recording actual position of the target using Global positioning system (GPS) of a smartphone, as the target moved from start point (denoted by START P(i) or Y(i), "i" denoting the path sequence) as shown in Figure 5. Sound Navigation & Ranging (SONAR) measurements were then taken to record the range and bearing of the target between the start point START P(i) and end point END P(i). To ensure sparsity of the scenario, the ranging paths were spread apart denoted by dotted yellow lines, namely, Y1, Y2, Y3, Y4 and Y5, and the dotted pink lines, namely, P1, P2 and P3. For computational convenience, the start point for all the three pink paths were kept the same. For a given target along one of the paths, the neighbor nodes were assumed to be taken at the rest of the paths, distributed randomly.

The nomenclature of various schemes are outlined as follows:

- Proposed method called Compressed-Sensing Malicious-node Compensation (abbreviated as CS-MC)
- Triangulation method (abbreviated as C-TOL) [25]
- Forward Scan Sonar- Forward Seabed Elevation estimation technique (abbreviated as FSS-FSE) [7]
- Fusion of unscented Kalman filter and Linear Kalman filter for joint estimation of target (abbreviated as UL-KF fusion) [5]

Triangulation method [25] uses the concept of triangulation uncertainty to determine the localization error of estimated position. FSS-FSE technique [7] uses an acoustic approach in the form of Sonar Scan readings in the two dimensional underwater domain to estimate the distribution of seabed

FIGURE 5. Target trajectory in a realistic UASN scenario.

elevation. UL-KF algorithm [5] jointly estimates underwater positioning as well as sea drift with the fusion of Kalman filter in positioning as well as sea drift with the fusion of Kalman filter in case of multiple ranging. The performance metrics are explained in brief as follows:

i Localization error: It is defined as the norm of the error in positioning decided by actual coordinates and the estimated coordinates, given by the formula: $L.E = mean\left(\sqrt{(\alpha_x - \hat{\alpha}_x)^2 + (\alpha_y - \hat{\alpha}_y)^2}\right)$ for actual node positions (α_x, α_y) and estimated node positions $(\hat{\alpha}_x, \hat{\alpha}_y)$.

ii Localization ratio: This parameter is defined as the number of targets localized to the total number of targets. If $a.n_\rho$ denotes the number of anchor nodes and α is the position of target, then the frequency of $(L.E) < 1m$ denotes successful retrieval of target for a given set of measurements from neighboring nodes.

iii Correlation function of actual and measured parameter: Sparsity is affected by the amount of correlation in possessed by the neighboring nodes and the target.

iv The Bias norm of target coordinates α is given by the formula

$$Bias = \left\| \frac{\sum_{iter=1}^{\max} \hat{\alpha}_{iter}}{iter_{\max}} - \boldsymbol{\alpha} \right\| \tag{45}$$

where, $\hat{\alpha}_{iter}$ denotes the triangulated position of the target using m^{th} or n^{th} UAN or USN, respectively, $\boldsymbol{\alpha}$ denotes the actual coordinates of the target and the number of passes is given by $iter$.

A. DISCUSSION

1) LOCALIZATION ERROR

Localization error for the proposed scheme and the compared methods is shown in Figure 6. The localization error due to the proposed method is up to 20.69% lower than FSS-FSE and up to 70.34% lower than UL-KF fusion method or the triangulation method. CS-MC achieves lower localization error because of the ability to sense a sparsely deployed scenario followed by discretization of grid vector which enables easier categorization of target's whereabouts. In the next set of standard comparisons, Figure 7 demonstrates the distribution of positioning errors in terms of the x-coordinate and the y-coordinate for different path-trajectories in the form of scatter-plots while employing the proposed CS-MC technique. It may be observed that most of the positioning errors are negligible because the plots are centered around zero on the x-axis. However, the y-axis plots are spread between $+2$ and -2 m, indicating that positioning is more prone to error along the longitude if the anchor nodes are positioned laterally beside the target position. Paths Y2, Y4 and Y5 are positively skewed whereas path Y3 is negatively skewed. Path Y1 shows negligible skewness, attributed to the presence of anchor nodes which are completely non-overlapping with the target trajectory, leading to uniform probability of positive as well as negative errors. Skewness can be attributed to positive or negative value of insertion vector coefficient. According to Lemma 3.1.b, positive skewness denotes malicious behavior in a subtractive sense, while negative skewness is an indication of abundance of additive sense of maximum possible malice. In either case, the insertion function $\mathbf{V}(\alpha)$ remains bounded as per equation (35). To denote the effect of Distance of the target and the anchor nodes from stationary position on the localization accuracy, a percentage error plot is presented in Figure 8. In absence of any acoustic stratification, the fitness function of the insertion matrix coefficients a and b, given by $U(\alpha)$ undergoes Bregman's Projection optimization, which results in reduction of percentage error in positioning by 17.15% at a separation distance of 200m, 29.95% at 400m, 45.61% at 600m, 42.46% at 800m before tapering off to 5.08% at 1000m and 0.21% at 1200m as compared to conventional insertion vector. It may also be observed that effect of sparse sensing based localization is profound up to 800m, but beyond that, the rate of localization failure increases rapidly, which is more of a physical limitation rather than the limitation of the proposed technique.

2) LOCALIZATION RATIO

Localization ratio is the ratio of the number of successful attempts to the total number of attempts at localization in a sensor node deployment scenario. Successful localization attempt is counted as the one where the localization error is less than the threshold. In present context, three thresholds are shown: namely error $<$ 1 m, error $<$ 2 m and error $<$3 m. As observed from the graph of Figure 9a, localization ratio peaks at 75 hits for an insertion coefficient variance of 1.995 and 58 hits for 2.512, using the proposed method. In comparison, the FSS-FSE method manages 63 hits at $\sigma^2 = 1.99$ and 48 hits at $\sigma^2 = 2.512$ which is lower than CS-MC by 16% and 17.24%, respectively. The performance of UL-KF fusion is lower than CS-MC by 20% and 18.96%, respectively. In Figure 9b, once the tolerance for error is relaxed from $<$ 1 m to $<$ 2 m, it is observed

that successful localization is achieved for a wider range of insertion coefficient variations. Consequently, a non-zero hit is observed for 1.259, 1.584, 1.995, 2.512, 3.162, 3.981 and 5.011, as compared to fewer variances of Figure9a. After further relaxing the error bound, number of successful hits saturates to 124 for $\sigma^2 = 1.259$ to $\sigma^2 = 5.011$, while extending towards $\sigma^2 = 6.309$ before tapering off to zero for higher variances.

3) CORRELATION FUNCTION

The cross-correlation between insertion matrix when the target is on path Y with that of path P, is also calculated and shown in Figure 10. For a distance of 1242 m from the start position, path Y1 and P1 experiences peak correlation, indicating difficulty in compressive sensing due to degradation of sparsity between the node and the target. The reason could be attributed to the weak fulfilment of equation (15) of Corollary 2.1.a, resulting in a weak search space $\boldsymbol{\eta}$. In comparison, paths Y2 and P2 experience a correlation which is lower by 13.25% at its peak. Further reduction of 8.84% and 9.93% is observed for correlations of paths Y3 and P3 (abbreviated from now on as (Y3,P3)) and paths (Y4,P4), respectively, as compared to the correlation of path (Y2,P2), which indicates stronger fulfilment of the search space $\boldsymbol{\eta}$ as mentioned in equation (13) of Corollary 2.1.a.

Underwater paths performance is determined by cross correlation of multiple paths Y1, Y2, Y3, Y4 and Y5, as shown in Figure 11. The correlation peaks at 1.69 for paths (Y3,Y5) at 398m and 952m, followed by 1.64 at 1535m for paths (Y1,Y5). These points represent the worst-case scenario for CS-MC algorithm and all other path trajectories follow a similar pattern with peaks at more than one point. If just the peaks are considered, then (Y1,Y5) is safer than (Y3,Y5) by 3.24%. The possibility of estimated locations matching with the discrete lattice points is the lowest for (Y3,Y5), followed by an increase of 3.24% for (Y1,Y5), 5.01% for (Y2,Y5), 10.74% for (Y3,Y4), 15.17% for (Y1,Y4), 16.58% for (Y2,Y4), 27.86% for (Y1,Y3) etc.

The contour plot of insertion vector $\mathbf{V}(\alpha)$ is given in Figure 12. The coefficients a and b of insertion vector $\mathbf{V}(\alpha)$ are moderately negative for Y5 path measurements, denoted by dark blue contours of moderate radius. For localization to take place successfully, the alignment of insertion coefficient with lattice framework is crucial according to equation (16) of Proposition 2.2.a. However, to satisfy the restricted isometry property (RIP), if the insertion function is made non-continuous, then number of hits with a given polarity (positive or negative) would be useful metric that would quantify the contours of Figure 12. Therefore, deeper blue would mean more negative bias of the insertion function coefficient, whereas lighter yellow would indicate positive bias of insertion coefficients. Contours of large radius would indicate more number of coefficients with the specified polarity, and smaller radius would indicate fewer number of coefficients of the insertion function of CS-MC. As observed from the Figure 12, paths Y3 and P2 demonstrate distinct positive bias.

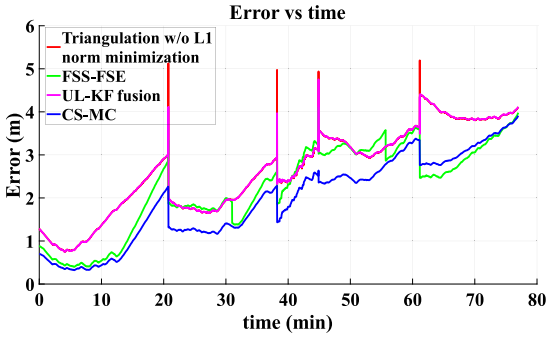

FIGURE 6. Localization performance in terms of absolute positioning error.

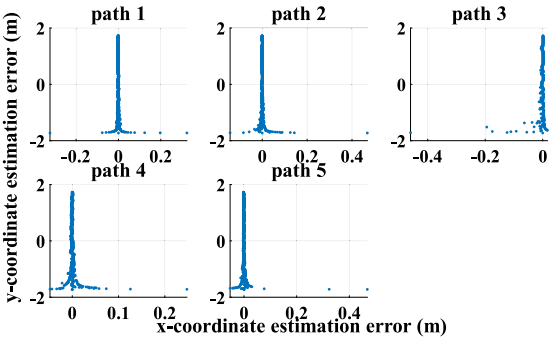

FIGURE 7. Scatter plot of positioning error using CS-MC technique.

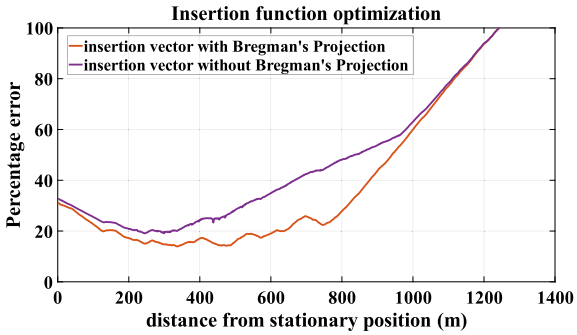

FIGURE 8. Error in estimating the insertion vector as a function of anchor node distance.

Path Y5 on the other hand, exhibits inclination towards negative valued coefficients. Extremes of coefficients appear more and more as the source to destination distance is increased.

4) BIAS NORM

A bias plot is computed in Figure 13 for various path trajectories using the proposed CS-MC method. Using Bregman's projection method, the alignment of estimation coefficients is the closest to the ideal fitness function of equation (40) for Path Y3 followed by Y5. Consequently, the bias is the least for Y3 as compared to other paths. Precisely, CS-MC presents a reduction of 68.06%, 23.49%, 21.72% and 15.93% over the worst case scenario, by paths Y3, Y5, Y4 and Y2, respectively.

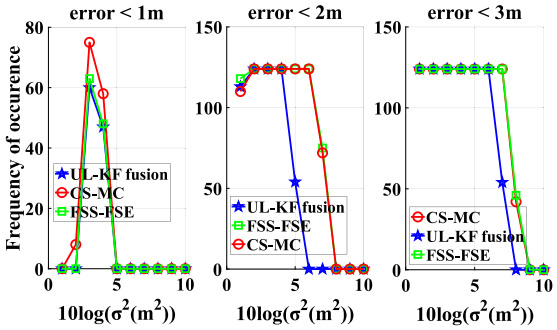

FIGURE 9. Localization ratio with varying tolerance of error (a) less than 1m, (b) less than 2m, (c) less than 3m.

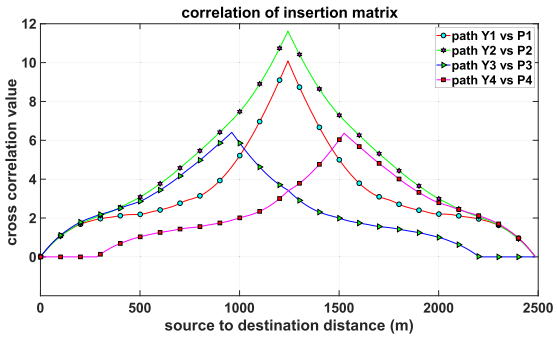

FIGURE 10. Cross-correlation function for multiple path trajectories.

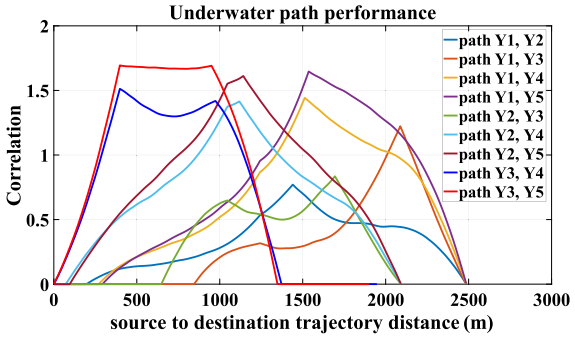

FIGURE 11. Correlation of trajectories as a function of source to destination distance.

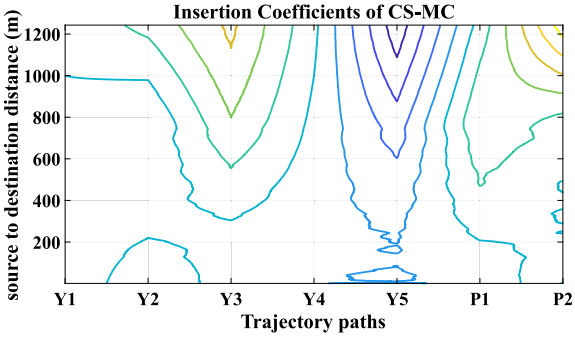

FIGURE 12. Contour plot of insertion coefficients for different target trajectories.

To observe how erroneous estimation piles up with successive measurements, cumulative Bias is plotted

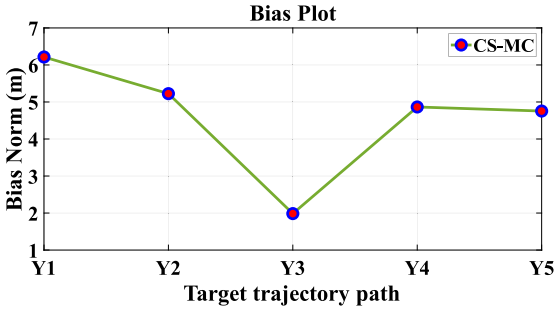

FIGURE 13. Bias plot of the proposed method for different target trajectories.

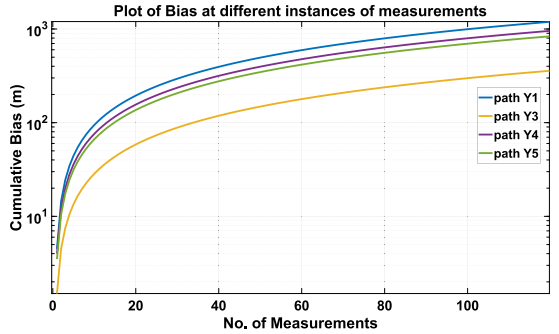

FIGURE 14. Cumulative Bias of CS-MC method as a function of number of measurements.

in Figure 14 for paths Y1 though Y5. Once again, Y3 racks up the lowest set of errors, followed by Y5. This gives us a glimpse into future improvements to the proposed work by reducing the cumulative effect of errors in case of underwater sparse retrieval of location information. In terms of cumulative Bias, the proposed method posts a savings of 69.9%, 29.82% and 19.79% by paths Y3, Y5 and Y4, respectively, over the worst case scenario.

V. CONCLUSION

The authors established a compressed-sensing based localization framework for estimating the target position in a malicious and acoustically stratified medium with the help of the proposed CS-MC Theorem. Compared to the unstratified acoustic path, the proposed method achieved improved localization performance of at least 20.69% and a reduction of percentage error by at least 17.15% up to 800m distance of separation in terms of insertion vector. For the malicious types discussed in the present context, the proposed method exhibit lower node-metastasis by at least 16%. Incoherence was measured and found to be improved up to 27.86% over the conventional techniques, which meant that the CS-MC Theorem could trap estimated positions more efficiently even under node duress. Considering the fitness of the estimation coefficients, the CS-MC method promised an upliftment of at least 15% over the worst-case counterpart. Based on these observations, the authors in the present work expect that the proposed method using CS-MC model can effectively

counter malicious effects of underwater acoustic nodes and compensate for localization errors even in the presence of node metastasis, as proven in Lemma 3.1.a-c. In the upcoming work, further analysis shall be attempted in sparse node geometries to achieve AUV-assisted compressed sensing and acoustic positioning.

APPENDIX

There is no appendix.

REFERENCES

[1] Z. Xiong, M. Wu, J. Cao, Y. Liu, R. Yu, and S. Cai, "An underwater gravimetry method using inertial navigation system and depth gauge based on trajectory constraint," *IEEE Geosci. Remote Sens. Lett.*, vol. 18, no. 9, pp. 1510–1514, Sep. 2020, doi: 10.1109/lgrs.2020.3005153.

[2] J. Wang, T. Zhang, B. Jin, Y. Zhu, and J. Tong, "Student's T-based robust Kalman filter for a SINS/USBL integration navigation strategy," *IEEE Sensors J.*, vol. 20, no. 10, pp. 5540–5553, May 2020, doi: 10.1109/JSEN.2020.2970766.

[3] J. Guo, D. Li, and B. He, "Intelligent collaborative navigation and control for AUV tracking," *IEEE Trans. Ind. Informat.*, vol. 17, no. 3, pp. 1732–1741, Mar. 2021, doi: 10.1109/TII.2020.2994586.

[4] P. Stinco, A. Tesei, G. Ferri, S. Biagini, M. Micheli, B. Garau, K. D. LePage, L. Troiano, A. Grati, and P. Guerrini, "Passive acoustic signal processing at low frequency with a 3-D acoustic vector sensor hosted on a buoyancy glider," *IEEE J. Ocean. Eng.*, vol. 46, no. 1, pp. 283–293, Jan. 2021, doi: 10.1109/JOE.2020.2968806.

[5] J. Kim, "Cooperative localization and unknown currents estimation using multiple autonomous underwater vehicles," *IEEE Robot. Autom. Lett.*, vol. 5, no. 2, pp. 2365–2371, Apr. 2020, doi: 10.1109/LRA.2020.2972889.

[6] P. Paral, A. Chatterjee, and A. Rakshit, "Human position estimation based on filtered sonar scan matching: A novel localization approach using DENCLUE," *IEEE Sensors J.*, vol. 21, no. 6, pp. 8055–8064, Mar. 2021, doi: 10.1109/JSEN.2020.3048396.

[7] J. Pyo, H. Cho, and S.-C. Yu, "On-site calibration-based estimation method of forward seabed elevation using forward scan sonar," *IEEE Sensors J.*, vol. 19, no. 19, pp. 8832–8844, Oct. 2019, doi: 10.1109/JSEN.2019.2918512.

[8] L. Chen, S. Wang, H. Hu, D. Gu, and L. Liao, "Improving localization accuracy for an underwater robot with a slow-sampling sonar through graph optimization," *IEEE Sensors J.*, vol. 15, no. 9, pp. 5024–5035, Sep. 2015, doi: 10.1109/JSEN.2015.2432082.

[9] W. Zhang, G. Han, X. Wang, M. Guizani, K. Fan, and L. Shu, "A node location algorithm based on node movement prediction in underwater acoustic sensor networks," *IEEE Trans. Veh. Technol.*, vol. 69, no. 3, pp. 3166–3178, Mar. 2020, doi: 10.1109/TVT.2019.2963406.

[10] Y. Zhang, X. Liu, M. Luo, and C. Yang, "Bio-inspired approach for long-range underwater navigation using model predictive control," *IEEE Trans. Cybern.*, vol. 51, no. 8, pp. 4286–4297, Aug. 2019, doi: 10.1109/tcyb.2019.2933397.

[11] W. Erb, "Shapes of uncertainty in spectral graph theory," *IEEE Trans. Inf. Theory*, vol. 67, no. 2, pp. 1291–1307, Feb. 2021, doi: 10.1109/TIT.2020.3039310.

[12] Y. Zhang, Y. Li, Y. Zhang, and T. Jiang, "Underwater anchor-AUV localization geometries with an isogradient sound speed profile: A CRLB-based optimality analysis," *IEEE Trans. Wireless Commun.*, vol. 17, no. 12, pp. 8228–8238, Dec. 2018, doi: 10.1109/TWC.2018.2875432.

[13] T. Northardt, "A Cramér-rao lower bound derivation for passive sonar track-before-detect algorithms," *IEEE Trans. Inf. Theory*, vol. 66, no. 10, pp. 6449–6457, Oct. 2020, doi: 10.1109/TIT.2020.3013991.

[14] W. Yan, X. Fang, and J. Li, "Formation optimization for AUV localization with range-dependent measurements noise," *IEEE Commun. Lett.*, vol. 18, no. 9, pp. 1579–1582, Sep. 2014, doi: 10.1109/LCOMM.2014.2344033.

[15] L. Zhang, T. Zhang, H. S. Shin, and X. Xu, "Efficient underwater acoustical localization method based on time difference and bearing measurements," *IEEE Trans. Instrum. Meas.*, vol. 70, 2021, Art. no. 8501316, doi: 10.1109/TIM.2020.3045193.

[16] Z. Guan, H. Kulhandjian, and T. Melodia, "Stochastic channel access in underwater networks with statistical interference modeling," *IEEE Trans. Mob. Comput.*, vol. 20, no. 10, pp. 3020–3033, Oct. 2020, doi: 10.1109/tmc.2020.2993026.

[17] J. Haupt, R. M. Castro, and R. Nowak, "Distilled sensing: Adaptive sampling for sparse detection and estimation," *IEEE Trans. Inf. Theory*, vol. 57, no. 9, pp. 6222–6235, Sep. 2011, doi: 10.1109/TIT.2011.2162269.

[18] S. Chen and X. Feng, "Cramer-rao bounds for the joint delay-Doppler estimation of compressive sampling pulse-Doppler radar," *J. Syst. Eng. Electron.*, vol. 29, no. 1, pp. 58–66, Feb. 2018, doi: 10.21629/JSEE.2018.01.06.

[19] H. Cao, Y. T. Chan, and H. C. So, "Efficient sensing for compressive estimation of frequency of a real sinusoid," *IEEE Trans. Aerosp. Electron. Syst.*, vol. 57, no. 1, pp. 744–750, Feb. 2020, doi: 10.1109/TAES.2020.3015322.

[20] K. You, W. Guo, Y. Liu, W. Wang, and Z. Sun, "Grid evolution: Joint dictionary learning and sparse Bayesian recovery for multiple off-grid targets localization," *IEEE Commun. Lett.*, vol. 22, no. 10, pp. 2068–2071, Oct. 2018, doi: 10.1109/LCOMM.2018.2863374.

[21] M. Guo, Y. D. Zhang, and T. Chen, "DOA estimation using compressed sparse array," *IEEE Trans. Signal Process.*, vol. 66, no. 15, pp. 4133–4146, Aug. 2018, doi: 10.1109/TSP.2018.2847645.

[22] H. Fu and Y. Chi, "Quantized spectral compressed sensing: Cramér–Rao bounds and recovery algorithms," *IEEE Trans. Signal Process.*, vol. 66, no. 12, pp. 3268–3279, Jun. 2018.

[23] Y. Gu and N. A. Goodman, "Information-theoretic compressive sensing kernel optimization and Bayesian Cramér–Rao bound for time delay estimation," *IEEE Trans. Signal Process.*, vol. 65, no. 17, pp. 4525–4537, Sep. 2017, doi: 10.1109/TSP.2017.2706187.

[24] A. Abtahi, S. Gazor, and F. Marvasti, "Off-grid localization in MIMO radars using sparsity," *IEEE Signal Process. Lett.*, vol. 25, no. 2, pp. 313–317, Feb. 2018, doi: 10.1109/LSP.2018.2791447.

[25] Prateek and R. Arya, "C-TOL: Convex triangulation for optimal node localization with weighted uncertainties," *Phys. Commun.*, vol. 46, Jun. 2021, Art. no. 101300, doi: 10.1016/j.phycom.2021.101300.

[26] Prateek, R. Arya, and A. K. Verma, "Non-coherent localization with geometric topology of wireless sensor network under target and anchor node perturbations," *Wireless Netw.*, vol. 27, no. 3, pp. 2271–2286, Apr. 2021, doi: 10.1007/s11276-021-02575-5.

[27] C. B. Song and S. T. Xia, "Sparse signal recovery by ℓ_q minimization under restricted isometry property," *IEEE Signal Process. Lett.*, vol. 21, no. 9, pp. 1154–1158, Oct. 2014, doi: 10.1109/LSP.2014.2323238.

[28] A. Nalci, I. Fedorov, M. Al-Shoukairi, T. T. Liu, and B. D. Rao, "Rectified Gaussian scale mixtures and the sparse non-negative least squares problem," *IEEE Trans. Signal Process.*, vol. 66, no. 12, pp. 3124–3139, Jun. 2018, doi: 10.1109/TSP.2018.2824286.

[29] C. Wu and J. Elangage, "Multiemitter two-dimensional angle-of-arrival estimator via compressive sensing," *IEEE Trans. Aerosp. Electron. Syst.*, vol. 56, no. 4, pp. 2884–2895, Aug. 2020, doi: 10.1109/TAES.2019.2958397.

[30] R. Boyer, R. Couillet, B.-H. Fleury, and P. Larzabal, "Large-system estimation performance in noisy compressed sensing with random support of known cardinality—A Bayesian analysis," *IEEE Trans. Signal Process.*, vol. 64, no. 21, pp. 5525–5535, Nov. 2016, doi: 10.1109/TSP.2016.2591511.

[31] Z. Pan, Q. Zhu, G. Liang, and H. Hu, "Coverage probability and average rate of uplink cellular networks based on a 3-D model," *Chin. J. Electron.*, vol. 27, no. 5, pp. 1098–1103, Sep. 2018, doi: 10.1049/cje.2018.06.017.

[32] R. Bhatia, *Matrix Analysis*. New York, NY, USA: Springer-Verlag, 1997.

[33] D. S. Friedlander, "Parameter estimation," *Int. LISREL*, vol. 61, no. 20, pp. 55–81, 2004.

[34] H. Sundar, T. V. Sreenivas, and C. S. Seelamantula, "TDOA-based multiple acoustic source localization without association ambiguity," *IEEE/ACM Trans. Audio, Speech, Language Process.*, vol. 26, no. 11, pp. 1976–1990, Nov. 2018, doi: 10.1109/TASLP.2018.2851147.

[35] Z. Wang, X. Ma, R. Chen, S. Zhang, and G. R. Arce, "Fast pixelated lithographic source and mask joint optimization based on compressive sensing," *IEEE Trans. Comput. Imag.*, vol. 6, pp. 981–992, 2020, doi: 10.1109/TCI.2020.3000010.

PRATEEK (Graduate Student Member, IEEE) received the B.Tech. degree in electronics and communication engineering (ECE) from SPSU, Udaipur, India, in 2014, and the M.Tech. degree in communication system engineering from the Kalinga Institute of Industrial Technology (KIIT), Bhubaneswar, India, in 2017. He is currently pursuing the Ph.D. degree with the Department of Electronics and Communication Engineering, National Institute of Technology Patna, Bihar, India. His research interests include wireless communication and soft computing techniques.

KUNDAN KUMAR is currently pursuing the Ph.D. degree with the Department of Electronics and Communication Engineering, National Institute of Technology Patna, Bihar, India. His research interests include wireless sensor networks and optimization techniques.

KRISHNA PANDEY received the B.Tech. degree in electronics and communication engineering (ECE) from UPTU Lucknow, India, in 2008, and the M.Tech. degree in information and communication technology (specialization in wireless communication and network) from the School of ICT, Gautam Buddha University, Greater Noida, India, in 2012. He is currently pursuing the Ph.D. degree with the Department of Electronics and Communication Engineering, National Institute of Technology Patna, Bihar, India. His research interests include device to device (D2D) communication and 5G Internet of Things.

SAURABH CHANDRA (Graduate Student Member, IEEE) received the B.E. degree in ETC from Chhattisgarh Swami Vivekanand Technical University (CSVTU), Bhilai, India, in 2014, and the M.Tech. degree in communication system engineering from the Kalinga Institute of Industrial Technology (KIIT), Bhubaneswar, India, in 2017. He is currently a Research Fellow with the Department of Electronics and Communication Engineering, National Institute of Technology Patna, Bihar, India. His research interests include wireless communication and device to device communication.

RAJEEV ARYA (Member, IEEE) received the Engineering degree in electronics and communication engineering from the Government Engineering College, Ujjain, (RGPV University, Bhopal), India, in 2008, the M.Tech. degree in electronics and communication engineering from the Indian Institute of Technology (ISM), Dhanbad, India, in 2012, and the Ph.D. degree in communication engineering from the Indian Institute of Technology (IIT Roorkee), Roorkee, India, in 2016. He is currently an Assistant Professor with the Department of Electronics and Communication Engineering, National Institute of Technology Patna, India. His current research interests include communication systems and wireless communication. He received the Ministry of Human Resource Development Scholarship (MHRD India) during his M.Tech. and Ph.D. degrees.